Solid phase epitaxy of diamond cubic Sn_xGe_{1-x} alloys

M. E. Taylor,[a] G. He, and Harry A. Atwater
Thomas J. Watson Laboratories of Applied Physics, California Institute of Technology, Pasadena, California 91125

A. Polman
FOM Institute for Atomic and Molecular Physics, Kruislaan 407, 1098 SJ Amsterdam, The Netherlands

(Received 9 May 1996; accepted for publication 15 July 1996)

Solid phase epitaxy of amorphous Sn_xGe_{1-x} films on strain relieved Ge films on Si(001) substrates was investigated for alloy compositions in the range $0.02 \leqslant x \leqslant 0.26$. Films with compositions $x < 0.05$ crystallize by solid phase epitaxy as substitutional, strain relieved, diamond cubic alloys without phase separation or surface segregation of Sn. Films with higher Sn compositions exhibit more complicated behavior in which phase separation is believed to follow solid phase epitaxy. This sequence of transformations for higher Sn compositions yields epitaxial, substitutional, strain relieved, diamond cubic Sn_xGe_{1-x} films with $x \sim 0.05$, and excess Sn is segregated in ~100 nm size domains within the epitaxial alloy film. © *1996 American Institute of Physics.* [S0021-8979(96)06220-2]

I. INTRODUCTION

Synthesis of group IV semiconductor alloys for use in Si-based heterostructures is now expanding beyond the original work on Si_xGe_{1-x} alloys[1] to include C_xSi_{1-x},[2] $(C_xGe_{1-x})_ySi_{1-y}$,[3,4] $(C_xSn_{1-x})_ySi_{1-y}$,[5] and Sn_xGe_{1-x} alloys.[6–17] Electronic structure calculations predict that the binary alloy Sn_xGe_{1-x} is a direct energy gap semiconductor with a gap that ranges between 0.55 and 0 eV as the composition is varied between $x=0.2$ and $x=0.8$.[18–21] Recent infrared spectroscopy measurements of the absorption coefficient indicate that the direct energy gap of Sn_xGe_{1-x} ranges between 0.8 and 0.25 eV as the composition is varied between $x=0$ and $x=0.15$.[22] Sn_xGe_{1-x} also has potential for monolithic integration on Si substrates. As a result, Sn_xGe_{1-x} is of interest for future Si-based infrared optoelectronics applications.

The synthesis of Sn_xGe_{1-x} alloy films has been the subject of previous investigations with growth by solid phase recrystallization,[6–8] sputtering,[9] molecular beam epitaxy,[10–14] ion assisted molecular beam epitaxy,[15,16] and pulsed laser deposition.[17] Unfortunately, Sn and Ge form a simple eutectic with mutual solid solubilities of less than 1%.[23–26] As a result, conventional thermal growth leads to severe Sn surface segregation. Ion assisted molecular beam epitaxy and pulsed laser deposition have produced epitaxial films with compositions falling in the range believed to be necessary for direct gap material. However, these growth methods are conceptually and practically more complicated than solid phase epitaxy, which is already widely employed in silicon integrated circuit technology. In the present work, Sn_xGe_{1-x} alloy growth by solid phase epitaxy was studied to explore the kinetics of segregation and to determine the composition limits achievable by this simple growth process. Previous reports of the kinetics of Ge solid phase epitaxy[27–29] and Si_xGe_{1-x} solid phase epitaxy[30,31] provided the context for this work.

[a]Electronic mail: maggie@daedalus.caltech.edu

II. EXPERIMENT

Amorphous Sn_xGe_{1-x} alloy films were deposited by ultrahigh vacuum molecular beam deposition on cleaned Si(001) substrates. Prior to growth, desorption of the surface hydrogen from the Si(001) surface was performed at 550 °C. The substrate temperature was subsequently lowered to 400 °C for deposition of a strain relieved heteroepitaxial Ge(001) layer (*c*-Ge), and to 70 °C for deposition of amorphous Ge (*a*-Ge) and amorphous Sn_xGe_{1-x} (*a*-Sn_xGe_{1-x}) layers. Four sample compositions were investigated: (1) 170 nm *a*-$Sn_{0.02}Ge_{0.98}$/10 nm *a*-Ge/60 nm *c*-Ge/Si(001), (2) 170 nm *a*-$Sn_{0.10}Ge_{0.90}$/70 nm *a*-Ge/20 nm *c*-Ge/Si(001), (3) 170 nm *a*-$Sn_{0.19}Ge_{0.81}$/100 nm *c*-Ge/Si(001), and (4) 190 nm *a*-$Sn_{0.26}Ge_{0.74}$/70 nm *a*-Ge/10 nm *c*-Ge/Si(001).

Following isothermal vacuum anneals, film compositions and microstructures were characterized by 300 keV transmission electron microscopy and high resolution x-ray diffraction using Cu $K\alpha_1$ radiation and the (400) diamond cubic peak. In the electron and x-ray diffraction analysis, the virtual crystal approximation was assumed. The electron diffraction patterns were used to identify the crystal orientations, and the differences in lattice parameter between Si and Sn_xGe_{1-x} reflections were used to estimate the compositions of the annealed films. The presence of (400) peaks in x-ray diffraction and the angular positions of these peaks relative to the Si substrate peak were also used to identify the crystal orientations and to estimate the film compositions, providing an independent confirmation of the structure and composition information.

Two MeV He^{++} Rutherford backscattering spectra were obtained before and after anneals to provide information about film composition, film microstructure, and growth kinetics of solid phase epitaxy. The preanneal and postanneal random spectra were compared to identify changes in the Sn depth profile and Ge surface energy indicative of Sn surface segregation. The preanneal and postanneal channeling spectra were compared to identify changes in amorphous layer thickness, from which crystal–amorphous interface velocities were calculated.

 0021-8979/96/80(8)/4384/5/$10.00

To obtain additional information about solid phase epitaxial growth kinetics, time-resolved reflectivity measurements were performed using either a 5 mW continuous-wave GaAs diode laser operating at 825 nm or a 5 mW continuous-wave InGaP diode laser operating at 670 nm. Laser irradiation was focused on the sample surface at near-normal incidence, and the reflected intensity was measured with a Si photodetector over the course of an anneal. In time-resolved reflectivity, the film thickness corresponding to one reflectivity oscillation is given by $\lambda/2n$, where λ is the laser wavelength and n is the index of refraction of the film. Dividing the thickness corresponding to one oscillation by the time needed to complete one oscillation yields the interface velocity. Since data on the refractive index of Sn_xGe_{1-x} alloys are not available, the index values were taken as 4.64 and 5.21, the reported values for crystalline Ge at 825 and 670 nm, respectively.[32]

In solid phase epitaxy, interface velocities ideally exhibit an Arrhenius temperature dependence $v = v_0 e^{-Q/kT}$, where v_0 is a pre-exponential velocity and Q is an activation energy for interfacial rearrangement processes in crystallization. Values for the pre-exponential velocity and activation energy were calculated from Arrhenius plots of the interface velocities obtained from the Rutherford backscattering and time-resolved reflectivity measurements. For Ge, pre-exponential velocities and activation energies of 1.2×10^9 cm/s, 2.0 eV, 2.17 ± 0.20 eV, and 2.26 ± 0.02 eV have been reported.[27–29]

III. RESULTS

Figure 1 is a cross-sectional transmission electron micrograph of a partially crystallized epitaxial $Sn_{0.02}Ge_{0.98}$ film annealed at 360 °C for 40 min. It illustrates several interesting microstructural features. Dislocations, stacking faults, and twins are visible at the interfaces between Si and Ge and between Ge and $Sn_{0.02}Ge_{0.98}$, as expected for strain relieved, lattice mismatched layers. The crystal–amorphous interface is characterized by pits (i.e., local minima in the crystal thickness) located at the exit points of threading dislocations. Previously, in solid phase epitaxy of Si_xGe_{1-x}, the crystal–amorphous interface was observed to roughen by formation of {111} facets, a phenomenon attributed to strain relaxation.[30] While the interface pits observed in this work resemble {111} facets, it is unlikely that their formation is related to misfit strain relaxation, since full strain relaxation was most likely achieved through the crystallographic defects that occurred earlier in the solid phase epitaxy process. The ⟨110⟩ electron diffraction pattern exhibits a spot separation consistent with epitaxial, substitutional, strain relieved, diamond cubic $Sn_{0.02}Ge_{0.98}$, which is confirmed by the x-ray data of Fig. 2(a), collected from a film annealed at 360 °C for 70 m. Rutherford backscattering spectra were obtained from films annealed at 300 and 325 °C. The spectra shown in Fig. 2(b) correspond to a partially crystallized alloy annealed at 300 °C for 14 h. The Sn profiles in the preanneal and post-anneal random spectra overlap exactly, indicating that no surface segregation of Sn occurred during the anneals. The channeling spectra yielded interface velocities which, when plotted against temperature, gave values for the pre-exponential velocity and solid phase epitaxy activation energy of 1×10^{11} cm/s and 2.38 eV. In both the Sn and Ge profiles, channeling minimum yields of approximately 50% were observed, which is consistent with the high density of crystallographic defects arising from lattice mismatch. The time-resolved reflectivity data of Fig. 3(a) were collected at 350, 375, 400, and 425 °C. These spectra show a slight decrease in the reflectivity amplitude as compared to published spectra for pure Ge.[28] This is consistent with the rough crystal–amorphous interface observed in Fig. 1. Interface velocities were calculated and plotted against temperature, giving values for the pre-exponential velocity and solid phase epitaxy activation energy of $8 \times 10^9 - 3 \times 10^{10}$ cm/s and 2.30 ±0.04 eV, respectively.

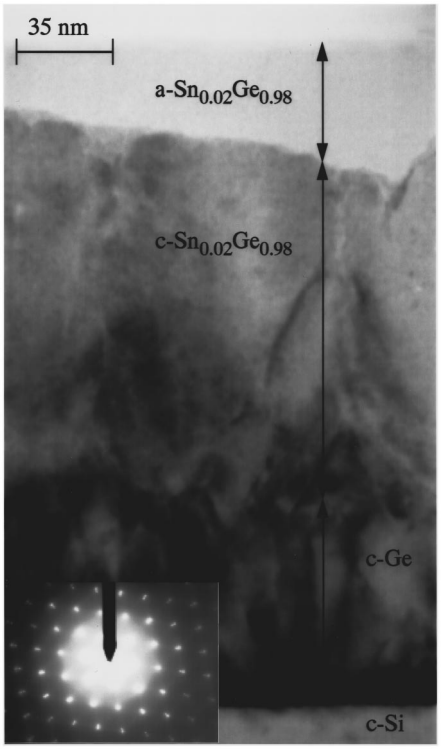

FIG. 1. Cross-sectional transmission electron micrograph of a partially crystallized $Sn_{0.02}Ge_{0.98}$ alloy annealed at 360 °C for 40 min. Crystallographic defects arising from lattice mismatch are visible at the Si and Ge interface and at the Ge and $Sn_{0.02}Ge_{0.98}$ interface. Pits in the crystal–amorphous interface resemble {111} facets, and correspond to the exit points of threading dislocations. The ⟨110⟩ diffraction pattern indicates that the annealed film is an epitaxial, substitutional, strain relieved, diamond cubic $Sn_{0.02}Ge_{0.98}$ alloy.

For the annealed $Sn_{0.10}Ge_{0.90}$ alloy, plan view transmission electron microscopy in combination with energy dispersive x-ray spectroscopy shows a Sn_xGe_{1-x} film with low Sn content, obscured by roughly circular regions of Sn approximately 60 nm in diameter. The ⟨001⟩ diffraction pattern exhibits a spot separation indicative of epitaxial, substitutional, strain relieved, diamond cubic $Sn_{0.05}Ge_{0.95}$. No spots or rings corresponding to the Sn regions were observed. The time-resolved reflectivity data of Fig. 3(b) were collected at 390, 455, and 505 °C. As before, a decrease in the reflectivity amplitude is apparent, indicating loss of interface planarity. Qualitatively, the traces are very similar to the traces observed for the $Sn_{0.02}Ge_{0.98}$ alloy. However, after the final

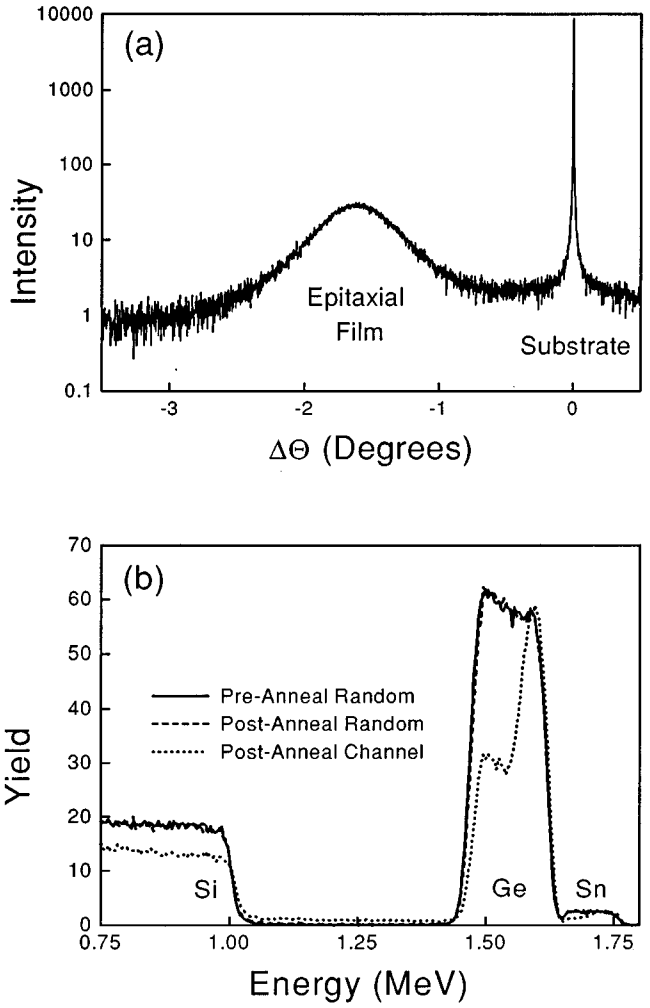

FIG. 2. (a) High resolution Cu $K\alpha_1$ x-ray diffraction data and (b) 2 MeV He^{++} Rutherford backscattering spectrometry data for annealed $Sn_{0.02}Ge_{0.98}$ alloys. In (a), the sample was annealed at 360 °C for 70 min. The position of the (400) x-ray peak is consistent with epitaxial, substitutional, strain relieved, diamond cubic $Sn_{0.02}Ge_{0.98}$. In (b), the sample was annealed at 300 °C for 14 h, and is not completely crystallized. The random spectra show no change in the Sn profile or in the Ge edge energy, indicating that no Sn surface segregation occurred. The channeling spectrum shows equal minimum yields in the Sn and Ge, suggesting that no Sn phase separation occurred.

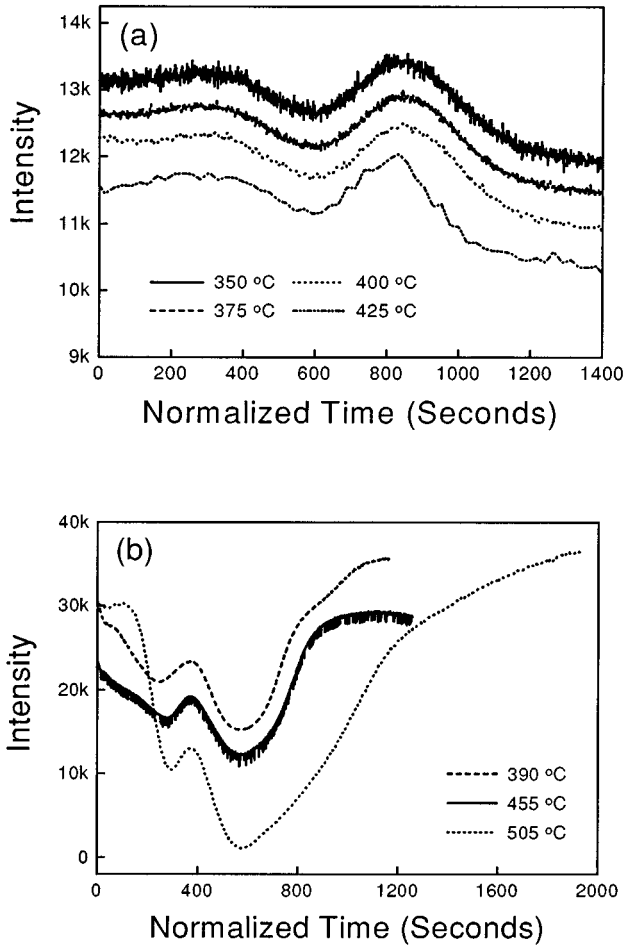

FIG. 3. Time-resolved reflectivity measurements at $\lambda=825$ nm for (a) $Sn_{0.02}Ge_{0.98}$ and (b) $Sn_{0.10}Ge_{0.90}$. In (a), the traces are indicative of solid phase epitaxy characterized by a rough interface. In (b), the traces are indicative of solid phase epitaxy as described in (a), possibly followed by surface segregation of Sn.

reflectivity minimum that corresponds to completion of solid phase epitaxial crystallization, the reflection intensities in the $Sn_{0.10}Ge_{0.90}$ traces rise smoothly into plateaus. Since Sn has a higher reflectivity than Ge, Sn surface segregation could lead to increased reflection intensity. A possible explanation is that there was a time delay between the completion of crystallization and the onset of phase separation resulting from a difference in the activation energies for solid phase epitaxy and phase separation. Such a delay was observed previously for polycrystalline $Sn_{0.25}Ge_{0.75}$ grown by solid phase crystallization on amorphous substrates.[8] This result implies that, by a very careful choice of the anneal time, $Sn_{0.10}Ge_{0.90}$ might be grown by solid phase epitaxy without phase separation. However, if the annealing time is too long, the Sn phase separates, leaving behind an epitaxial $Sn_{0.05}Ge_{0.95}$ film. Interface velocities were calculated and plotted against temperature, giving values for the pre-exponential velocity and solid phase epitaxy activation energy of 6×10^{-5}–10 cm/s and 0.77 ± 0.38 eV, respectively.

Figure 4(a) is a plan view transmission electron micrograph of a $Sn_{0.19}Ge_{0.81}$ alloy annealed at 300 °C for 60 min. It indicates that the microstructure of annealed $Sn_{0.19}Ge_{0.81}$ is very similar to that observed for annealed $Sn_{0.10}Ge_{0.90}$. The Sn regions are approximately 400 nm in diameter. As in the case of annealed $Sn_{0.10}Ge_{0.90}$, the ⟨001⟩ diffraction pattern exhibits a spot separation indicative of epitaxial, substitutional, strain relieved, diamond cubic $Sn_{0.05}Ge_{0.95}$. Figure 4(b) are Rutherford backscattering spectra collected before and after an anneal at 325 °C for 42 min. Comparison of the Sn profiles in the preanneal and postanneal random spectra indicates that Sn surface segregation occurred. The leading edge of the Ge peak in the postanneal spectrum is at a lower energy than in the preanneal spectrum, also indicating that some Sn surface segregation occurred. However, this change in the Ge edge is not large enough to suggest complete surface segregation of Sn. Rather, it indicates that less than 10% of the phase separated Sn is at the surface. Postanneal channeling spectra exhibit minimum yields of approximately 50%

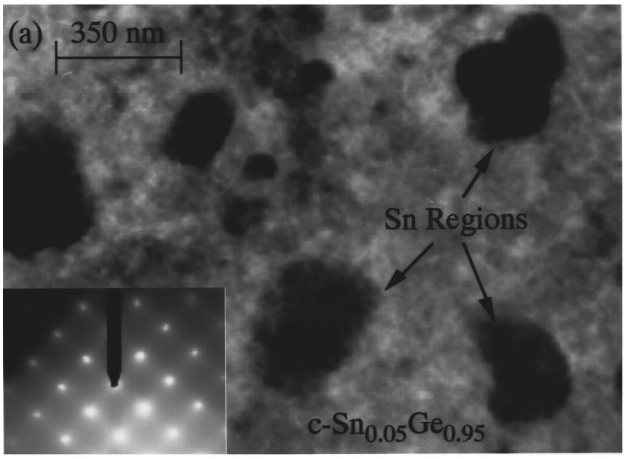

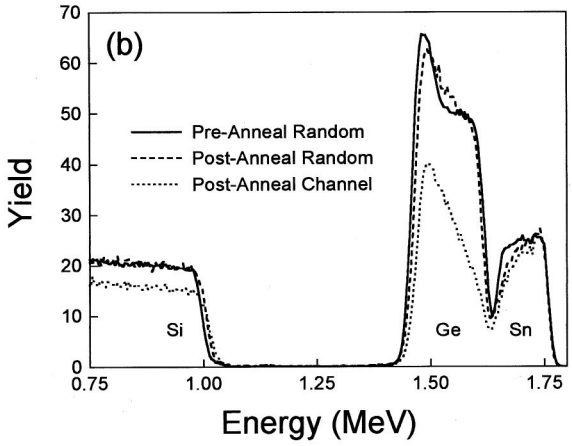

FIG. 4. (a) Plan view transmission electron micrograph and (b) 2 MeV He^{++} Rutherford backscattering spectrometry data for annealed $Sn_{0.19}Ge_{0.81}$ alloys. In (a), the sample was annealed at 300 °C for 60 min. The image shows dark regions identified as Sn by energy dispersive x-ray spectroscopy, indicating Sn phase separation. The diffraction pattern is that of an epitaxial, substitutional, strain relieved, diamond cubic $Sn_{0.05}Ge_{0.95}$ alloy. In (b), the sample was annealed at 325 °C for 42 min. The change in the Sn profile and the offset in the Ge surface energy between the preanneal and postanneal random spectra indicate that some Sn surface segregation occurred. However, the offset is not large enough to account for all Sn not incorporated into the epitaxial film, suggesting that most of the phase separated Sn remained in the body of the film. The difference between the Ge and Sn minimum yield is also suggestive of Sn phase separation.

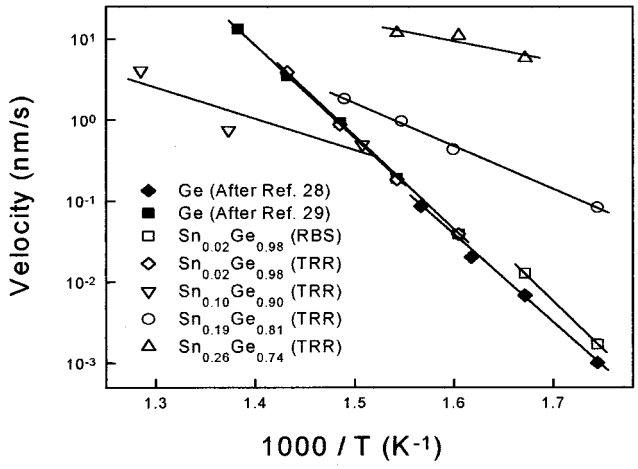

FIG. 5. Arrhenius plot of interface velocities obtained from the Rutherford backscattering spectrometry and time-resolved reflectivity measurements. For Ge, pre-exponential velocities of 1.2×10^9 cm/s and solid phase epitaxy activation energies of 2.0, 2.17±0.20, and 2.26±0.02 eV have been reported (Refs. 27–29). For the $Sn_{0.02}Ge_{0.98}$ alloy, Rutherford backscattering and time-resolved reflectivity give pre-exponential velocities of 1×10^{11} and 8×10^9–3×10^{10} cm/s and solid phase epitaxy activation energies of 2.38 and 2.30±0.04 eV, respectively. For the $Sn_{0.10}Ge_{0.90}$ alloy, time-resolved reflectivity gives a pre-exponential velocity of 6×10^{-5}–10 cm/s and a solid phase epitaxy activation energy of 0.77±0.38 eV. For the $Sn_{0.19}Ge_{0.81}$ alloy, time-resolved reflectivity gives a pre-exponential velocity of 7–30 cm/s and an apparent activation energy of 1.05±0.04 eV. For the $Sn_{0.26}Ge_{0.74}$ alloy, time-resolved reflectivity gives a pre-exponential velocity of 2×10^{-4}–0.3 cm/s and an apparent activation energy of 0.48±0.20 eV.

and 90% in the Ge and Sn profiles, respectively, which is a further indication of Sn phase separation within the body of the film. Time-resolved reflectivity data were collected at 300, 352, 373, and 398 °C. Although oscillations were observed, they were not characteristic of solid phase epitaxy. Instead, the reflectivity intensity increased monotonically to a constant value for each anneal temperature, which can be attributed to Sn surface segregation. A short time delay, required to align the laser, occurred between the start of the anneal and the start of data collection. It is possible that no oscillations corresponding to solid phase epitaxy were observed because solid phase epitaxy was completed before data collection began. This explanation would imply a time lag between completion of crystallization and onset of phase separation, as possibly observed in the case of the $Sn_{0.10}Ge_{0.90}$ alloy. It is also possible that no oscillations corresponding to solid phase epitaxy were observed because phase separation occurred concurrently with solid phase epitaxy, destroying the interface planarity. This second explanation is unlikely, considering that an epitaxial film resulted. It is not clear whether an appropriately short annealing time would enable solid phase epitaxy without phase separation. If a time interval exists between these processes, it is clearly very short. Interface velocities were calculated from the observed oscillations and plotted against temperature to give values for the pre-exponential velocity and apparent activation energy of 7–30 cm/s and 1.05±0.04 eV, respectively.

For the annealed $Sn_{0.26}Ge_{0.74}$ alloy, plan view transmission electron microscopy reveals a microstructure very similar to those observed for the annealed $Sn_{0.10}Ge_{0.90}$ and $Sn_{0.19}Ge_{0.81}$ alloys, with Sn regions approximately 600 nm in diameter. As in the previous two cases, the ⟨001⟩ pattern and spot separations are indicative of epitaxial, substitutional, strain relieved, diamond cubic $Sn_{0.05}Ge_{0.95}$, and x-ray diffraction confirms this observation. Time-resolved reflectivity data were collected at 325, 350, and 375 °C, and a monotonic reflectivity increase indicative of Sn segregation, as in the previous alloy composition, was observed. Interface velocities were calculated and plotted against temperature to give values for the pre-exponential velocity and apparent activation energy of 2×10^{-4}–0.3 cm/s and 0.48±0.20 eV, respectively.

IV. CONCLUSIONS

In summary, solid phase epitaxy of diamond cubic Sn_xGe_{1-x} from amorphous Sn_xGe_{1-x} layers with Sn fraction

less than $x \sim 0.05$ is possible without evidence of phase separation. The crystal–amorphous interface in alloy solid phase epitaxy appears to be considerably rougher than that observed for solid phase epitaxy of pure Ge. In alloys of higher Sn fraction, phase separation occurs, leaving an epitaxial, substitutional, strain relieved, diamond cubic film with $x \sim 0.05$. For these alloys, some of the Sn segregates to the surface, but most of the phase separated Sn remains in the body of the film.

These results are surprising in light of a previous study of solid phase epitaxy in amorphous Si supersaturated with impurities including In, Bi, Ga, and Sn.[33] In that work, phase separation was observed to occur either before or concurrent with crystallization, probably driven by the lower solid solubilities of the impurities in crystalline Si than in amorphous Si. Polycrystalline Si films resulted. In this work, Ge supersaturated with at least twice the solid solubility of Sn crystallized epitaxially with no sign of phase separation. In alloys with higher Sn fractions where phase separation was observed, the resulting films are epitaxial Ge films supersaturated with at least five times the solid solubility of Sn. While other interpretations are certainly possible, the fact that epitaxial films are observed suggests that crystallization preceded phase separation.

Since recent absorption spectroscopy experiments suggest that Sn_xGe_{1-x} may have a band gap tunable over approximately 0.25 eV in the $x=0$ to $x=0.05$ composition range, solid phase epitaxy may prove to be an attractive and practical fabrication method for Sn_xGe_{1-x}/Ge heterostructures.[22]

ACKNOWLEDGMENTS

This work was supported by the National Science Foundation via Grant No. DMR-9503210. Work at the FOM Institute was made possible by financial support from the NATO Division of Scientific Affairs and Environmental Affairs, NWO, STW, and IOP Electro-Optics. C. Ahn and C. Garland are acknowledged for expert assistance with transmission electron microscopy.

[1] J C. Bean, T. T. Sheng, L. C. Feldman, A. T. Fiory, and R. T. Lynch, Appl. Phys. Lett. **44**, 102 (1984).
[2] S. S. Iyer, K. Eberl, M. S. Goorsky, F. K. Legoues, J. C. Tsang, and F. Cardone, Appl. Phys. Lett. **60**, 356 (1992).
[3] K. Eberl, S. S. Iyer, S. Zollner, J. C. Tsang, and F. K. Legoues, Appl. Phys. Lett. **60**, 3033 (1992).
[4] J. W. Strane, H. J. Stein, S. R. Lee, B. L. Doyle, S. T. Picraux, and J. W. Mayer, Appl. Phys. Lett. **63**, 2786 (1993).
[5] G. He, M. D. Savellano, and H. A. Atwater, Appl. Phys. Lett. **65**, 1159 (1994).
[6] S. Oguz, W. Paul, T. T. Deutsch, B. Y. Tsaur, and D. V. Murphy, Appl. Phys. Lett. **43**, 848 (1983).
[7] I. T. H. Chang, B. Cantor, and A. G. Cullis, J. Non-Cryst. Solids **117–118**, 263 (1990).
[8] S. M. Lee, J. Appl. Phys. **75**, 1987 (1994).
[9] S. I. Shah, J. E. Greene, L. L. Abels, Q. Yao, and P. M. Raccah, J. Cryst. Growth **83**, 3 (1987).
[10] A. Harwit, P. R. Pukite, J. Angilello, and S. S. Iyer, Thin Solid Films **184**, 395 (1990).
[11] J. Piao, R. Beresford, T. Licata, W. I. Wang, and H. Homma, J. Vac. Sci. Technol. B **8**, 221 (1990).
[12] H. J. Gossman, J. Appl. Phys. **68**, 2791 (1990).
[13] E. A. Fitzgerald, P. E. Freeland, M. T. Asom, W. P. Lowe, R. A. Macharrie, Jr., B. E. Weir, A. R. Kortan, F. A. Thiel, Y. H. Xie, A. M. Sergent, S. L. Cooper, G. A. Thomas, and L. C. Kimberling, J. Electron. Mater. **20**, 489 (1991).
[14] W. Wegscheider, J. Olajos, U. Menczigar, W. Dondl, and G. Abstreiter, J. Cryst. Growth **123**, 75 (1992).
[15] G. He and H. A. Atwater, Nucl. Instrum. Methods Phys. Res. B **106**, 126 (1995).
[16] G. He and H. A. Atwater, Appl. Phys. Lett. **68**, 664 (1996).
[17] M. E. Taylor, G. He, C. Saipetch, and H. A. Atwater, Mater. Res. Soc. Symp. Proc. **388**, 97 (1995).
[18] D. W. Jenkins and J. D. Dow, Phys. Rev. B **36**, 7994 (1987).
[19] B. I. Craig, Superlattices Microstruct. **12**, 1 (1992).
[20] H. A. Atwater, G. He, and K. Saipetch, Mater. Res. Soc. Symp. Proc. **355**, 123 (1995).
[21] E. Kaxiras (unpublished).
[22] G. He, R. Ragan, and H. A. Atwater (unpublished).
[23] T. Soma, H. Matsuo, and S. Kagaya, Phys. Status Solidi **105**, 311 (1981).
[24] T. B. Massalski, *Binary Alloy Phase Diagrams* (American Society of Metals, Metals Park, OH, 1986), Vol. 2.
[25] C. D. Thurmond, J. Chem. Phys. **57**, 827 (1953).
[26] C. D. Thurmond, F. A. Trumbore, and M. Kowalchik, J. Chem. Phys. **24**, 799 (1956).
[27] L. Csepregi, R. P. Küllen, J. W. Mayer, and T. W. Sigmon, Solid State Commun. **21**, 1019 (1977).
[28] G. Q. Lu, E. Nygren, M. J. Aziz, D. Turnbull, and C. W. White, Appl. Phys. Lett. **56**, 137 (1990).
[29] G. L. Olson and J. A. Roth, *Handbook of Crystal Growth*, edited by D. T. J. Hurle (Elsevier, Amsterdam, 1994), Vol. 3, pp. 257–312.
[30] D. C. Paine, D. J. Howard, N. G. Stoffel, and J. A. Horton, J. Mater. Res. **5**, 1023 (1990).
[31] P. Kringhoj and R. G. Elliman, Phys. Rev. Lett. **73**, 858 (1994).
[32] R. F. Potter, *Handbook of Optical Constants of Solids*, edited by E. D. Palik (Academic, Orlando, FL, 1985), p. 474.
[33] E. Nygren, J. C. McCallum, R. Thornton, J. S. Williams, and G. L. Olson, Mater. Res. Soc. Symp. Proc. **100**, 405 (1988).